Suppression of instability in liquid flow down an inclined plane by a deformable solid layer

V. Shankar* and Akhilesh K. Sahu
Department of Chemical Engineering, Indian Institute of Technology, Kanpur 208 016, India
(Received 27 August 2005; published 10 January 2006)

The linear stability of a liquid layer flowing down an inclined plane lined with a deformable, viscoelastic solid layer is analyzed in order to determine the effect of the elastohydrodynamic coupling between the liquid flow and solid deformation on the free-surface instability in the liquid layer. The stability of this two-layer system is characterized by two qualitatively different interfacial instability modes: In the absence of the deformable solid layer, the free surface of the liquid film undergoes a long-wave instability due to fluid inertia. With the presence of the deformable solid layer, the interface between the fluid and the solid undergoes a finite-wavelength instability when the deformable solid becomes sufficiently soft. The effect of the solid layer deformability on the free-surface instability of the liquid film flow is analyzed using a long-wave asymptotic analysis. The asymptotic results show that for a fixed Reynolds number and inclination angle, the free-surface instability is completely suppressed in the long-wave limit when the nondimensional (inverse) solid elasticity parameter $\Gamma=\overline{V_a}\eta/(GR)$ increases beyond a critical value. Here, $\overline{V_a}$ is the average velocity of the liquid film flow, η is the viscosity of the liquid, G is the shear modulus of the solid layer, and R is the thickness of the liquid layer. The predictions of the asymptotic analysis are verified and extended to finite wavelengths using a numerical solution, and this indicates that the suppression of the free-surface instability indeed continues to finite wavelength disturbances. Further increase of Γ is found to have two consequences: first, the interface between the liquid and the deformable solid layer could become unstable at finite wavelengths; second, the free-surface interfacial mode could also become unstable at finite wavelengths due to an increase in solid layer deformability. However, our numerical results demonstrate that, for a given average velocity, there exists a sufficient window in the value of shear modulus G where both the unstable modes are *absent at all wavelengths*. Our study therefore suggests that soft solid layer coatings could potentially provide a passive method of suppressing free-surface instabilities in liquid film flows.

DOI: 10.1103/PhysRevE.73.016301 PACS number(s): 47.20.−k

I. INTRODUCTION

The onset of instability in the flow of a liquid film down an inclined plane and the consequent nonlinear spatiotemporal dynamics engendered by the instability has been an extensively studied subject in fluid dynamics [1], beginning from the pioneering studies of Benjamin [2] and Yih [3]. Apart from being interesting from a fundamental standpoint, a clear understanding of instabilities in liquid film flows is relevant to applications ranging from coating processes, distillation and/or absorption equipment, and pulmonary fluid mechanics [4]. Yih [3] employed a long-wave asymptotic analysis and showed that the liquid flow down an inclined plane could become unstable to long-wave disturbances at a sufficiently low Reynolds number. In particular, for the case of a vertical plate, the flow is unstable at any nonzero Reynolds number. Once the flow becomes unstable, the instability manifests as gravity-driven free-surface waves at the liquid-gas interface. A large number of subsequent studies have analyzed the nonlinear evolution of these unstable waves, and an extensive summary of the theoretical and computational studies in this area can be found in [1]. A similar instability for viscoelastic liquid flow down an inclined plane has been analyzed by Shaqfeh *et al.* [5]. Recent studies have addressed the effect of surfactants on the free-surface instability, in the presence of additional interfacial shear, for both Newtonian [6] and viscoelastic [7] liquids. These studies show that, in addition to the free-surface instability, there is another "surfactant mode" which also becomes unstable due to a shear-induced Marangoni effect. There have also been several recent studies which are aimed at controlling the free-surface instability (see [8,9], and references therein). Lin *et al.* [8] studied the effect of in-plane horizontal oscillations (in the direction parallel to the flow) in the inclined plate on the free-surface instability using the Floquet theory. They showed that by use of appropriate amplitudes and frequencies of the forced oscillations, it is possible to suppress the free-surface instability of the liquid film flow. More recently, Jiang and Lin [9] studied the effect of horizontal oscillations on a two-layer liquid film flow. They showed that the onset of instability in this system can be suppressed in certain parameter regimes by imparting oscillations of appropriate amplitudes and frequencies. In other parametric regimes, they showed that it is possible to even enhance the instability in the liquid film flow. These studies have suggested "active methods" toward suppressing the free-surface instability, where forced oscillations of the inclined plate are used to suppress the instability.

In this paper, we study the stability of a liquid flow down an inclined plane lined with a soft viscoelastic solid layer (see Fig. 1), in order to examine whether the deformability in the solid layer can suppress the free-surface instability. If indeed the deformable solid layer can suppress the free-surface instability, then this would represent a "passive" ap-

*Corresponding author; Electronic address: vshankar@iitk.ac.in

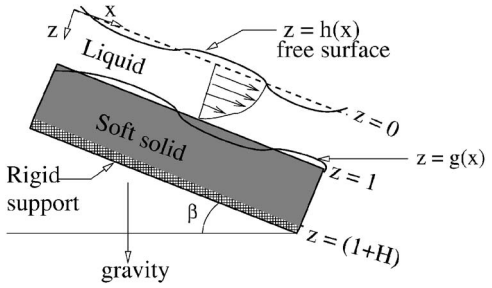

FIG. 1. Schematic diagram illustrating the system configuration and nondimensional coordinate system: a Newtonian liquid layer flowing past a deformable solid layer under the influence of gravity.

proach to controlling such instabilities, without any constant forcing such as oscillations. When a viscous liquid flows past a soft solid layer (shear modulus $\sim 10^4-10^6$ Pa), the normal and tangential stresses exerted by the fluid at the fluid-solid interface are sufficient to cause deformation in the solid layer, which in turn affects the adjacent fluid flow. Previous studies [10,11] have shown that this *elastohydrodynamic* coupling can destabilize liquid-solid interfaces and lead to the formation of interfacial waves. In this study, we ask the question of whether this elastohydrodynamic coupling can affect the free-surface instability in liquid flow down an inclined plane, and specifically, whether the free-surface instability can be completely suppressed by the presence of the solid layer. A previous study [12] on the effect of a deformable solid layer on the two-layer plane Couette flow of two different Newtonian liquids has shown that in certain configurations (depending on the viscosity ratio of the two liquids and thickness ratio), the solid layer could have a stabilizing effect on the two-fluid interfacial instability. That study provides further motivation to examine the present configuration of liquid flow down an inclined plane lined with a deformable solid layer. In addition, the configuration of liquid flow down an inclined plane lined with a deformable solid layer is perhaps more readily realized in experiments when compared to the two-liquid configuration that was studied in [12]. In a slightly different context, the phenomenon studied here could also be relevant to biological flows such as flow in the airways of the lung, involving deformable conduits with liquid linings [4].

The rest of this paper is structured as follows: The governing equations, base state, and linear stability analysis are presented in Sec. II A–II C. In Sec. III, we carry out a long-wave asymptotic analysis to examine the effect of the deformable solid layer on the free-surface instability of the liquid flow. This is followed by a numerical study in Sec. IV which extends the long-wave asymptotic predictions to finite wavelengths. We finally conclude in Sec. V by summarizing the salient results from the present study, and also by discussing the implications of the present results to experimental investigations.

II. MATHEMATICAL FORMULATION

A. Governing equations

The system of interest (see Fig. 1) consists of a linear viscoelastic solid of thickness HR, shear modulus G, and viscosity η_w strongly bonded to a rigid surface at $z^*=(1+H)R$, a layer of Newtonian liquid of thickness R in the adjacent region $0<z^*<R$ flowing under the influence of gravity. The liquid layer is exposed to a passive gas at the free-surface $z^*=0$. The angle of inclination made by the rigid surface with the horizontal is denoted by β. Under laminar flow conditions, the solid layer is at rest, and the liquid film undergoes a steady unidirectional flow in the x direction, with a velocity distribution [3]:

$$\bar{v}_x^*(z^*) = \frac{\rho g \sin\beta}{2\eta}(R^2 - z^{*2}). \tag{1}$$

Here, ρ is the density of the liquid, η is its viscosity, g is acceleration due to gravity, and all dimensional variables are denoted with a superscript *. The cross-sectional average velocity of the laminar flow is given by $\overline{V_a} = \rho g R^2 \sin\beta/(3\eta)$. It is useful to nondimensionalize various physical quantities at the outset, and the following scales are used to this end: the average velocity of the laminar flow $\overline{V_a}$ is used for velocities, the thickness of the fluid R is used for lengths and displacements, $R/\overline{V_a}$ for time, and $\eta\overline{V_a}/R$ for stresses and pressure. Thus, H is the nondimensional thickness of the solid layer.

The nondimensional governing equations for the liquid flow are, respectively, the Navier-Stokes mass and momentum equations:

$$\partial_z v_z + \partial_x v_x = 0, \tag{2}$$

$$\mathrm{Re}[\partial_t + v_x\partial_x + v_z\partial_z]v_x = -\partial_x p + 3 + \nabla^2 v_x, \tag{3}$$

$$\mathrm{Re}[\partial_t + v_x\partial_x + v_z\partial_z]v_z = -\partial_z p + 3\cot\beta + \nabla^2 v_z, \tag{4}$$

where $\partial_t \equiv \partial/\partial t$ and similar definitions hold for ∂_x and ∂_z. Here, we consider only two-dimensional disturbances in the x-z plane, and hence we neglect the velocity and variations in the third (y) dimension. Thus, $\nabla^2=(\partial_x^2+\partial_z^2)$ is the Laplacian operator in two dimensions. The Reynolds number in the momentum equations is defined as $\mathrm{Re}=\rho\overline{V_a}R/\eta$. The terms 3 and 3 cot β, respectively, in the x and z momentum equations are due to the gravitational body force in the fluid. The total stress tensor $T_{ij}=-p\delta_{ij}+\tau_{ij}$ $(i,j=x,z)$ in the liquid is given by a sum of an isotropic pressure p and a deviatoric shear stress tensor τ_{ij}, and $\tau_{ij}=(\partial_i v_j+\partial_j v_i)$ for the Newtonian liquid of interest in this study. The interface $z=h(x)$ is exposed to a gas, and hence is treated as a "free surface" where the shear stress in the liquid vanishes. The normal stresses in the liquid at $z=h(x)$ must equal the hydrostatic pressure in the gas adjacent to it. The dynamical evolution of the free interface position $h(x)$ is governed by the kinematic condition to be applied at $z=h(x)$:

$$\partial_t h + v_x\partial_x h = v_z. \tag{5}$$

The deformable solid layer is modeled as an incompressible linear viscoelastic solid [13] following the previous studies [10,14,15] in flow past deformable solid surfaces. A recent study by Gkanis and Kumar [16] on the stability of the *single*-layer plane Couette flow of a Newtonian fluid past a deformable solid has examined the role of nonlinear rheo-

logical properties in the solid by modeling the deformable solid using the neo-Hookean model. This study shows that for nonzero interfacial tension between the fluid and the solid medium, and sufficiently large values of solid layer thickness ($H \geqslant 2$), the results from both linear and nonlinear solid models agree quite well, while for smaller values of solid thickness, the linear model somewhat overpredicts the critical velocity required for destabilizing the flow. It is demonstrated later in this paper that the linear viscoelastic model is expected to yield accurate results for the present study, and hence we employ this simple model to describe the deformation in the solid layer.

The dynamics of the solid layer is described by a displacement field u_i which represents the deviation of material points in the solid from their base-state positions. The velocity field in the solid layer is given by $v_i = \partial_t u_i$. In an incompressible solid, the displacement field satisfies the solenoidal condition

$$\partial_i u_i = 0. \tag{6}$$

The nondimensional momentum conservation equation in the solid is given by

$$\mathrm{Re}\, \partial_t^2 u_i = \partial_j \Pi_{ij} + \frac{\hat{g}_i}{\sin \beta}, \tag{7}$$

where $\Pi_{ij} = -p_g \delta_{ij} + \sigma_{ij}$ is the total stress tensor in the solid layer which is given by a sum of isotropic pressure p_g and a deviatoric stress σ_{ij}, $\hat{g}_i$ is a unit vector pointing in the direction of gravity. The density of the solid is assumed to be equal to the density of the liquid without loss of generality. If the densities were different, then the ratio of solid to liquid densities ρ_s/ρ_l will appear in the left side of the above equation. The low-wave-number ($k \ll 1$) asymptotic analysis carried out in Sec. III shows that, to leading order in the analysis, inertial stresses in the solid are $O(k^2)$ smaller than the elastic stresses, and the inertial stresses of the solid layer do not appear in the low-wave-number limit. Therefore the low-wave-number asymptotic results are expected to be valid for any value of the ratio ρ_s/ρ_l. At finite wave numbers, the inertial stresses could become comparable to the elastic stresses in the solid layer, and in such cases, there will be some quantitative difference in the results when the ratio $\rho_s/\rho_l \neq 1$. However, the qualitative predictions of the present study are expected to remain unaltered due to the change in density ratio. The deviatoric stress σ_{ij} is given by a sum of elastic and viscous stresses in the solid layer: $\sigma_{ij} = (1/\Gamma + \eta_r \partial_t)(\partial_i u_j + \partial_j u_i)$ where $\Gamma = \overline{V}_a \eta/(GR)$ is the nondimensional parameter characterizing the elasticity of the solid layer, and $\eta_r = \eta_w/\eta$ is the ratio of solid to fluid viscosities. A useful interpretation of Γ is that it is the estimated ratio of viscous shear stresses in the fluid to elastic stresses in the solid layer, and for a fixed set of $\overline{V}_a$, R, and η, $\Gamma \to 0$ in the limit of a rigid solid layer where the shear modulus G becomes very large ($\sim 10^{11}$ Pa). The solid layer is assumed to be perfectly bonded to the rigid surface at $z = (1+H)$, and so zero displacement conditions apply at this surface. The conditions at the interface $z = g(x)$ between the liquid and the solid layer are the continuity of velocities and stresses in the liquid and solid layers.

B. Base state

The base laminar state whose stability is of interest in this study is obtained by solving for the steady unidirectional flow in the x direction due to gravity, and the nondimensional velocity and pressure distribution in the fluid are given by

$$\bar{v}_x(z) = \tfrac{3}{2}(1 - z^2), \tag{8}$$

$$\bar{p}(z) = 3z \cot \beta, \tag{9}$$

where the base flow quantities are denoted by an overbar. The solid layer is at rest in this steady base state, but there is a nonzero unidirectional displacement $\bar{u}_x$ due to the liquid shear stresses at $z = 1$ and the body force

$$\bar{u}_x(z) = \frac{3\Gamma}{2}[(1+H)^2 - z^2], \tag{10}$$

$$\bar{p}_g(z) = 3z \cot \beta. \tag{11}$$

C. Linear stability analysis

The stability of the coupled fluid-solid system is examined using a linear stability analysis where small perturbations (denoted by primed quantities) are imposed to the fluid velocity field $v_i = \bar{v}_i + v_i'$ and other dynamical variables in the fluid and the solid layer are similarly perturbed. A temporal linear stability analysis is used to determine the evolution of these small perturbations to the base state. The perturbation quantities are expanded in the form of Fourier modes in the x direction, and with an exponential dependence in time:

$$v_i'(x,z,t) = \tilde{v}_i(z) \exp[\mathrm{i}k(x - ct)], \tag{12}$$

$$u_i'(x,z,t) = \tilde{u}_i(z) \exp[\mathrm{i}k(x - ct)], \tag{13}$$

where k is the wave number (inversely proportional to the wavelength) of perturbations, c is a complex wave speed that determines the growth of perturbations, and $\tilde{v}_i(z)$ and $\tilde{u}_i(z)$ are eigenfunctions which have to be determined from the linearized differential equations governing the stability. As mentioned earlier, only two-dimensional perturbations are considered here. The complex wave speed is written as $c = c_r + \mathrm{i}c_i$, where c_r denotes the phase velocity of perturbations, and c_i dictates the growth or decay of perturbations, and if $c_i > 0$ the given base state is temporally unstable.

The linearized equations governing the stability of the two-layer system are obtained by substituting the above expansions (12) and (13) in the governing equations (3)–(7), and linearization is carried out about the laminar base-state of interest (8). This yields the following equations for the liquid layer:

$$d_z \tilde{v}_z + \mathrm{i}k\tilde{v}_x = 0, \tag{14}$$

$$\mathrm{Re}[\mathrm{i}k(\bar{v}_x - c)\tilde{v}_x + (d_z \bar{v}_x)\tilde{v}_z] = -\mathrm{i}k\tilde{p} + (d_z^2 - k^2)\tilde{v}_x, \tag{15}$$

$$\mathrm{Re}[\mathrm{i}k(\bar{v}_x - c)\tilde{v}_z] = -d_z\tilde{p} + (d_z^2 - k^2)\tilde{v}_z. \tag{16}$$

The above equations can be combined to give a single fourth-order Orr-Sommerfeld equation [17]:

$$\mathrm{i}k\,\mathrm{Re}[(\bar{v}_x - c)(d_z^2 - k^2) - d_z^2\bar{v}_x]\tilde{v}_z = (d_z^2 - k^2)^2\tilde{v}_z. \tag{17}$$

The linearized stability equations for the displacement field in the solid layer are obtained similarly:

$$d_z\tilde{u}_z + \mathrm{i}k\tilde{u}_x = 0, \tag{18}$$

$$-\mathrm{Re}\,k^2c^2\tilde{u}_x = -\mathrm{i}k\tilde{p}_g + \left(\frac{1}{\Gamma} - \mathrm{i}kc\,\eta_r\right)(d_z^2 - k^2)\tilde{u}_x, \tag{19}$$

$$-\mathrm{Re}\,k^2c^2\tilde{u}_z = -d_z\tilde{p}_g + \left(\frac{1}{\Gamma} - \mathrm{i}kc\,\eta_r\right)(d_z^2 - k^2)\tilde{u}_z. \tag{20}$$

These equations can be combined to give a single fourth-order differential equation for $\tilde{u}_z$:

$$(1 - \mathrm{i}kc\,\eta_r\Gamma)(d_z^2 - k^2)^2\tilde{u}_z + \mathrm{Re}\,k^2c^2\Gamma(d_z^2 - k^2)\tilde{u}_z = 0. \tag{21}$$

The linearized kinematic condition describing the evolution of $\tilde{h}$, the Fourier expansion coefficient of $h(x,t) = \tilde{h}\exp[\mathrm{i}k(x-ct)]$, is obtained from (5)

$$\mathrm{i}k[\bar{v}_x(z=0) - c]\tilde{h} = \tilde{v}_z(z=0), \tag{22}$$

where all the dynamical quantities are linearized about the unperturbed interface $z=0$. The linearized boundary conditions at the unperturbed free-surface position $z=0$ are obtained by Taylor-expanding the boundary conditions about $z=0$ to give

$$-3\tilde{h} + (d_z\tilde{v}_x + \mathrm{i}k\tilde{v}_z) = 0, \tag{23}$$

$$-\tilde{p} - 3\tilde{h}\cot\beta + 2d_z\tilde{v}_z - k^2\Sigma\tilde{h} = 0. \tag{24}$$

The first of the above equations is the linearized tangential stress condition at the unperturbed free surface $z=0$, and the second equation is the linearized normal stress condition. Here, $\Sigma = \gamma/(\overline{V_a}\eta)$ is the nondimensional surface tension between the liquid and the gas, with γ being the dimensional surface tension. Note that in both the tangential and normal stress conditions, the process of linearization has given rise to additional contributions proportional to $-3\tilde{h}$, which couple the base laminar flow with the height fluctuations of the free interface.

The velocity and stress continuity conditions at the interface $z=g(x)$ between the liquid and the solid layer are also linearized [10] about the unperturbed interface at $z=1$ to give

$$\tilde{v}_z = -\mathrm{i}kc\tilde{u}_z, \tag{25}$$

$$\tilde{v}_x + d_z\bar{v}_x|_{z=1}\tilde{u}_z = -\mathrm{i}kc\tilde{u}_x, \tag{26}$$

$$(d_z\tilde{v}_x + \mathrm{i}k\tilde{v}_z) = \left(\frac{1}{\Gamma} - \mathrm{i}kc\,\eta_r\right)[d_z\tilde{u}_x + \mathrm{i}k\tilde{u}_z], \tag{27}$$

$$-\tilde{p} + 2d_z\tilde{v}_z = -\tilde{p}_g + 2\left(\frac{1}{\Gamma} - \mathrm{i}kc\,\eta_r\right)d_z\tilde{u}_z. \tag{28}$$

Here too, the interface conditions are linearized about the unperturbed interface $z=1$, and within the linear stability analysis, we have set the Fourier coefficient of the interfacial fluctuation $\tilde{g} = \tilde{u}_z(z=1)$. The second term in the left side of (26) represents a nontrivial contribution that arises as a result of Taylor-expansion of the velocity about the unperturbed interface. This contribution was shown to be responsible for destabilizing the fluid-solid interface by Kumaran *et al.* [10]. The boundary conditions for the displacement field at $z=(1+H)$ are simply zero displacement conditions:

$$\tilde{u}_z = 0, \quad \tilde{u}_x = 0. \tag{29}$$

This completes the specification of the stability problem for the two-layer configuration of interest here. The complex wave speed c is an unknown eigenvalue which is a function of Re, k, Γ, H, Σ, and η_r. For arbitrary values of k and Re, there is no closed-form analytical solution to the problem, and so the governing equations must be solved numerically in general. However, as first shown by Yih [3], liquid flow down an inclined plane becomes unstable in the long-wave limit, and a long-wave asymptotic analysis is therefore appropriate for the present problem as well.

III. LONG-WAVE ASYMPTOTIC ANALYSIS

In this section, we carry out a low wave number (i.e., long wavelength) asymptotic analysis for the case of liquid flow down an inclined plane lined with a deformable solid layer. Specifically, we focus on the effect of the solid layer deformability on the free-surface instability undergone by the liquid-gas interface. In order for the long-wave analysis to be valid, the wavelength of the disturbances must be large compared to all cross-stream widths, and, in general, k must satisfy $k \ll 1/(1+H)$. For $H \sim O(1)$, this implies $k \ll 1$, while in the limit $H \gg 1$, this implies $k \ll 1/H$. This suggests that for larger values of H, the long-wave analysis is valid at much smaller values of k. In the ensuing analysis, we consider solid-layer thickness $H \sim O(1)$, so we consider the low-wave-number limit $k \ll 1$, with $\mathrm{Re} \sim O(1)$ and $\Gamma \sim O(1)$, i.e., the parameters Re and Γ do not scale with the wave number in any particular way, and can be treated as arbitrary variables. This is required, since both Re and Γ are physical parameters that can be tuned as desired by changing the viscosity of the fluid, the shear modulus of the solid, the inclination angle, and the fluid density. We adapt Yih's [3] original long-wave analysis to the present problem, by modifying it to include the presence of the deformable solid layer. For $k \ll 1$, the complex wave speed is expanded in an asymptotic series in k:

$$c = c^{(0)} + kc^{(1)} + \cdots, \tag{30}$$

and in this study, it suffices to calculate the leading order and the $O(k)$ correction to c. We set $\tilde{v}_z \sim O(1)$, and this implies that $\tilde{v}_x \sim O(k^{-1})$ from the continuity equation (14), and $\tilde{p} \sim O(k^{-2})$ from the x-momentum equation (15). Thus, the ve-

locity and the pressure in the liquid layer are expanded as

$$\tilde{v}_z = \tilde{v}_z^{(0)} + k\tilde{v}_z^{(1)} + \cdots, \tag{31}$$

$$\tilde{v}_x = k^{-1}\tilde{v}_x^{(0)} + \tilde{v}_x^{(1)} + \cdots, \tag{32}$$

$$\tilde{p} = k^{-2}\tilde{p}^{(0)} + k^{-1}\tilde{p}^{(1)} + \cdots. \tag{33}$$

Subsequent analysis shows that it is sufficient to calculate only the leading order and the first correction to the dynamical variables in the liquid. The displacement and pressure fields in the solid layer are expanded in a similar fashion:

$$\tilde{u}_z = \tilde{u}_z^{(0)} + k\tilde{u}_z^{(1)} + \cdots, \tag{34}$$

$$\tilde{u}_x = k^{-1}\tilde{u}_x^{(0)} + \tilde{u}_x^{(1)} + \cdots, \tag{35}$$

$$\tilde{p}_g = k^{-2}\tilde{p}_g^{(0)} + k^{-1}\tilde{p}_g^{(1)} + \cdots. \tag{36}$$

The Fourier coefficient of the free-surface height fluctuation $\tilde{h}$ is also expanded in an asymptotic series, and $\tilde{h} \sim O(k^{-1})$ as can be seen from Eq. (22). We therefore have:

$$\tilde{h} = k^{-1}\tilde{h}^{(0)} + \tilde{h}^{(1)} + \cdots. \tag{37}$$

After substituting the above expansions in the governing stability equations for the liquid layer (14)–(17), we obtain the following differential equations governing the leading order and first correction to $\tilde{v}_z$:

$$d_z^4\tilde{v}_z^{(0)} = 0, \tag{38}$$

$$d_z^4\tilde{v}_z^{(1)} = \mathrm{i}\,\mathrm{Re}[(\bar{v}_x - c^{(0)})d_z^2\tilde{v}_z^{(0)} - (d_z^2\bar{v}_x)\tilde{v}_z^{(0)}]. \tag{39}$$

It turns out that the leading-order displacement field is sufficient in the present low-k analysis, and it is governed by the following differential equation:

$$d_z^4\tilde{u}_z^{(0)} = 0. \tag{40}$$

Next, we solve the leading-order problem and then the first correction in the following subsections.

A. Leading order

The governing equation for $\tilde{v}_z^{(0)}$ in the liquid layer is Eq. (38), and the equation for $\tilde{u}_z^{(0)}$ in the solid layer is Eq. (40). The boundary and interface conditions for the leading-order problem are obtained by substituting the asymptotic expansions in Eqs. (22)–(29). This results in the following conditions at $z=0$:

$$-3\tilde{h}^{(0)} + d_z\tilde{v}_x^{(0)} = 0, \tag{41}$$

$$-\tilde{p}^{(0)} = 0. \tag{42}$$

The leading-order conditions at the fluid-solid interface $z=1$ are given by

$$\tilde{v}_z^{(0)} = 0, \tag{43}$$

$$\tilde{v}_x^{(0)} = 0, \tag{44}$$

$$d_z\tilde{v}_x^{(0)} = \frac{1}{\Gamma}d_z\tilde{u}_x^{(0)}, \tag{45}$$

$$\tilde{p}^{(0)} = \tilde{p}_g^{(0)}. \tag{46}$$

The boundary conditions at $z=(1+H)$ are simply

$$\tilde{u}_z^{(0)} = 0, \quad \tilde{u}_x^{(0)} = 0. \tag{47}$$

An important consequence of the low-wave-number expansion for the interface conditions [Eqs. (25) and (26)] is that to leading order the fluid velocities $\tilde{v}_z^{(0)}$ and $\tilde{v}_x^{(0)}$ satisfy the no-slip conditions at $z=1$ as in a rigid boundary [Eqs. (43) and (44)]. This is because the right side of Eqs. (25) and (26) are $O(k)$ smaller than fluid velocities on the left side. This implies that the solid-layer deformability does not influence the leading-order fluid velocity field, and so the leading-order wave speed in the present problem must be identical to that of Yih's [3] analysis. However, the leading-order velocity field in the liquid layer exerts a shear stress on the solid layer via the tangential stress condition [Eq. (45)], and this causes a deformation in the solid layer at leading order. We now present the solution to the leading-order velocity and displacement fields, and the leading-order wave speed.

The general solution to differential equation (38) is simply

$$\tilde{v}_z^{(0)} = A_1 + A_2 z + A_3 z^2 + A_4 z^3. \tag{48}$$

Since the stability problem is linear and homogeneous, the eigenfunction $\tilde{v}_z$ is determined only up to a multiplicative constant, and without loss of generality we set $A_1=1$. Physically, this implies that we are normalizing the amplitude of the normal component of the liquid velocity at the free surface to be 1. After satisfying the leading-order boundary conditions [Eqs. (42)–(44)], we obtain the solution to the dynamical variables in the liquid layer as

$$\tilde{v}_z^{(0)} = (z-1)^2, \tag{49}$$

$$\tilde{v}_x^{(0)} = 2i(z-1), \tag{50}$$

$$\tilde{p}^{(0)} = 0. \tag{51}$$

Upon using the leading tangential stress condition at $z=0$ [Eq. (41)], we obtain $\tilde{h}^{(0)}=2\mathrm{i}/3$, and using the linearized kinematic condition (22), we obtain, to leading order

$$c^{(0)} = 3, \tag{52}$$

which is identical, as expected, to Yih's [3] result for liquid flow down an inclined rigid plane. Physically, this implies that the flow is neutrally stable to leading order, and therefore the first correction must be calculated in order to determine its stability. For subsequent analysis, we require the leading-order deformation field in the solid layer, and this is obtained by solving the differential equation (40):

$$\tilde{u}_z^{(0)} = B_1 + B_2 z + B_3 z^2 + B_4 z^3. \tag{53}$$

The constants are determined by the boundary conditions [Eqs. (45)–(47)] to give

$$\tilde{u}_z^{(0)} = \Gamma[z-(1+H)]^2, \tag{54}$$

$$\tilde{u}_x^{(0)} = 2i\Gamma[z-(1+H)], \tag{55}$$

$$\tilde{p}_g^{(0)} = 0. \tag{56}$$

With these solutions, we now proceed to calculate the first correction to the wave speed $c^{(1)}$.

B. First correction

The solution to the inhomogeneous differential equation (39) governing $\tilde{v}_z^{(1)}$ can be determined to be:

$$\tilde{v}_z^{(1)} = C_1 + C_2 z + C_3 z^2 + C_4 z^3 - \frac{i\,\mathrm{Re}}{20} z^5. \tag{57}$$

The constant C_1 can be set to zero since we have already fixed the amplitude of $\tilde{v}_z$ at $z=0$ to be 1 by setting $A_1=1$ at leading order. The other three constants are determined from the first correction to the boundary conditions at $z=1$ and $z=0$. These are obtained from Eqs. (22)–(25) as follows. At $z=0$, the first correction to the normal and tangential stress conditions become

$$-3\tilde{h}^{(1)} + d_z \tilde{v}_x^{(1)} = 0, \tag{58}$$

$$-\tilde{p}^{(1)} - 3\cot\beta \tilde{h}^{(0)} = 0. \tag{59}$$

At $z=1$, the first correction to the velocity continuity conditions become:

$$\tilde{v}_z^{(1)} = -\mathrm{i}c^{(0)}\tilde{u}_z^{(0)}, \tag{60}$$

$$\tilde{v}_x^{(1)} + d_z \bar{v}_x|_{z=1}\tilde{u}_z^{(0)} = -\mathrm{i}c^{(0)}\tilde{u}_x^{(0)}. \tag{61}$$

Note here that, in contrast to a rigid inclined surface, the deformation in the solid layer appears in the normal and tangential velocity conditions: *the leading-order deformation field in the solid layer affects the first correction to the fluid velocity field*. Using the conditions (59)–(61), the constants C_2, C_3 and C_4 are determined to give

$$\tilde{v}_z^{(1)} = \frac{-iz}{60}\{3[60\Gamma H(2+H-2z) + \mathrm{Re}(-1+z)^2(-7+2z+z^2)] + 20(-1+z)^2\cot\beta\}. \tag{62}$$

The effect of the solid-layer deformation appears in the above expression through the term proportional to ΓH. Using this result for $\tilde{v}_z^{(1)}$, the first correction to the height fluctuation $\tilde{h}^{(1)}$ can be calculated from Eq. (58) to give

$$\tilde{h}^{(1)} = -4\Gamma H + \tfrac{8}{15}\,\mathrm{Re} - \tfrac{4}{9}\cot\beta. \tag{63}$$

The first correction to the wave speed $c^{(1)}$ is then obtained from the first correction to the kinematic condition (22):

$$\mathrm{i}[\bar{v}_x(z=0) - c^{(0)}]\tilde{h}^{(1)} - \mathrm{i}c^{(1)}\tilde{h}^{(0)} = \tilde{v}_z^{(1)}(z=0). \tag{64}$$

In the above equation, all the quantities except $c^{(1)}$ are now calculated, so $c^{(1)}$ can be obtained as

$$c^{(1)} = i\left\{\left[\tfrac{6}{5}\,\mathrm{Re} - \cot\beta\right] - 9\Gamma H\right\}, \tag{65}$$

which is a purely imaginary quantity and hence dictates the stability of the system. The first term (inside square brackets) in the right side of the above equation is *identical* to Yih's [3] result (Eq. 37 of Yih's paper) for liquid flow down an inclined rigid surface. This term indicates that in a rigid inclined surface, when $\frac{6}{5}\,\mathrm{Re} > \cot\beta$, the free surface of the liquid layer undergoes a long-wave instability. The second term in the right side proportional to ΓH is due to the effect of the solid-layer deformability on the free-surface instability mode. Importantly, this term occurs with a *negative* sign meaning that the *solid layer always has a stabilizing effect on the free-surface instability*. It was previously noted that the parameter Γ represents the ratio of viscous stresses in the liquid to elastic stresses in the solid layer, and in the limit of a rigid solid layer, $\Gamma \to 0$. Clearly, in Eq. (65), the contribution from the deformable solid layer vanishes with $\Gamma \to 0$ (rigid solid layer limit), and when $H=0$ (no deformable solid layer; only the rigid wall present at $z=1$). However, for nonzero values of ΓH, the solid-layer deformability stabilizes the free-surface instability. In particular, the free-surface instability is completely stabilized in the long-wave limit if

$$9\Gamma H > (\tfrac{6}{5}\,\mathrm{Re} - \cot\beta). \tag{66}$$

Or, equivalently, in terms of the dimensional parameters that are present in Γ and Re, the above result translates into:

$$\frac{3\rho R H g}{G} > \frac{2\rho^2 R^3 g}{5\eta^2} - \frac{\cot\beta}{\sin\beta}, \tag{67}$$

in order for the free-surface instability to be stabilized in the long-wave limit. This is one of the central results of the present study. The present prediction of complete stabilization of the free-surface instability (in the long-wave limit) by the deformable solid layer is in marked contrast with the earlier study [12] on the effect of the solid layer on the two-layer plane Couette flow. There, the authors found that the solid layer contribution could be stabilizing or destabilizing depending on the thickness and viscosity ratio of the two liquids.

The first correction to the kinematic condition Eq. (64) provides some additional insight into the mechanism of the stabilization by the solid layer. We first note that the right side of Eq. (64) is zero, as can be seen from Eq. (62). Using Eq. (58) to eliminate $\tilde{h}^{(1)}$ in terms of $d_z\tilde{v}_x^{(1)}$, and using $\tilde{h}^{(0)} = 2i/3$, we obtain the result for $c^{(1)}$ as

$$c^{(1)} = \frac{3i}{4} d_z \tilde{v}_x^{(1)}|_{z=0}. \tag{68}$$

Thus, the first correction to the wave speed, which determines the stability of the free-surface mode, is directly related to the first correction to the shear stress in the liquid at the free surface. As pointed out in the preceding discussion, the destabilizing term due to fluid inertia (proportional to Re) appears only at the first correction to the fluid velocity field. In addition to this contribution, and in contrast to a rigid surface, the deformation in the soft solid layer creates a perturbation flow, which also appears at $O(k)$. If the perturbation

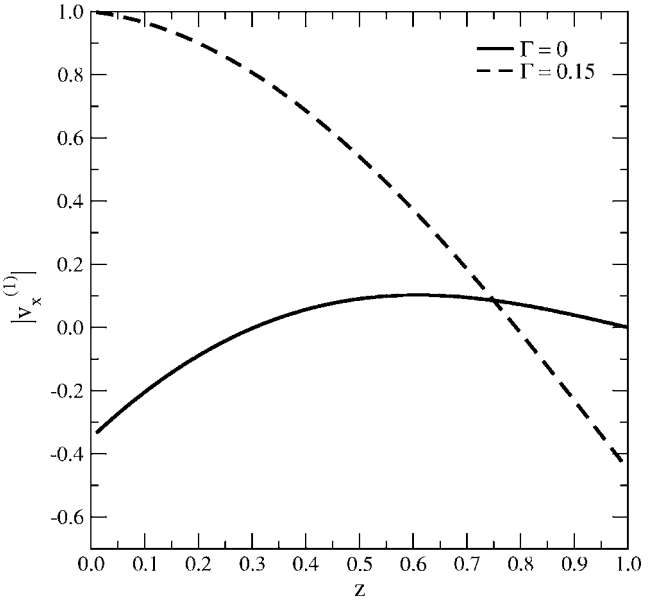

FIG. 2. Effect of solid layer deformability on the first correction to the eigenfunction: $|\tilde{v}_x^{(1)}|$ vs z for $\beta=\pi/2$, Re=1, $H=1$; $\Gamma=0$ and 0.15.

flow at $O(k)$ due to the solid deformation opposes the flow due to fluid inertia, then one would expect this to result in stabilization of the free-surface instability. Figs. 2 and 3 show representative plots of the x and z components of the first correction to the fluid velocity field, both for a rigid surface ($\Gamma=0$) and for a soft solid surface ($\Gamma=0.15$). These figures clearly demonstrate the qualitative change in the velocity profile for $\tilde{v}_x^{(1)}$ and $\tilde{v}_z^{(1)}$ due to the presence of the solid layer. In particular, $c^{(1)}$ is proportional to $d_z\tilde{v}_x^{(1)}|_{z=0}$, and this turns out to be negative in the presence of the soft layer,

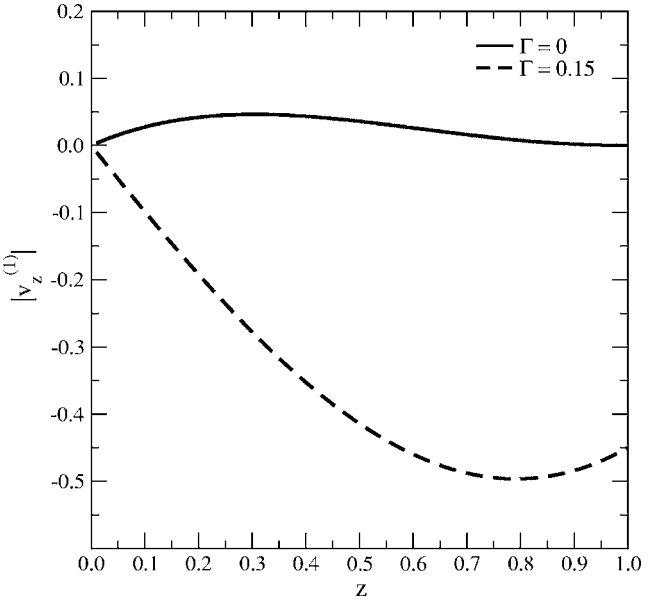

FIG. 3. Effect of solid layer deformability on the first correction to the eigenfunction: $|\tilde{v}_z^{(1)}|$ vs z for $\beta=\pi/2$, Re=1, $H=1$; $\Gamma=0$ and 0.15.

while it is positive for a rigid surface. This discussion clearly demonstrates that the perturbation flow created at $O(k)$ due to the deformation in the solid layer qualitatively alters the nature of the free-surface instability in the liquid layer.

We further note that in the low-k limit, the ratio of solid to liquid viscosity η_r and the liquid-gas surface tension Σ become subdominant, and hence do not appear in the above results. It is appropriate here to provide some estimates for the dimensional parameters in the problem so that the predicted suppression of the long-wave instability can be realized in an experiment. This is done using Eq. (67). Let us first consider the case $\beta=\pi/2$, $H=1$, $\rho=10^3$ kg/m^3, $g=9.8$ m/s^2, $G=10^4$ Pa, and $R=10^{-2}$ m. For $\beta=\pi/2$ (liquid film flowing vertically in the direction of gravity), $\cot(\pi/2)=0$, and so $9\Gamma H>\frac{6}{5}$ Re in order for the instability to be suppressed. For the above choice of dimensional parameters, we find that when $\eta\geqslant 11.55$ Pa s, then the predicted suppression can be realized in experiments. For $\beta=\pi/4$ (and all other parameters same as above), we require a critical Re in order for the instability to be present. Therefore, in this case we find the predicted suppression to be present if $1.6479<\eta<1.665$ Pa s. There is an upper limit because if the viscosity is too high, then the instability is not present in the first place in a rigid inclined surface. There is a lower limit because if the viscosity is too low, then for the shear modulus assumed (10^4 Pa), the solid layer cannot stabilize the long-wave instability. This discussion shows that it must be possible to experimentally realize the present predictions for flow of more viscous liquid films ($\eta\sim 1-10$ Pa s, $R\sim 1$ cm) down a soft elastomeric layer ($G\sim 10^4$ Pa).

If the predicted stabilization is to be realized in an experiment, it is not sufficient only if the long waves are stabilized by the deformable solid layer. Any arbitrary disturbance is expected to be composed of modes with all wavelengths, and so it is necessary to suppress the instability at all wavelengths. To this end, we extend our long-wave asymptotic results to finite wavelengths using a numerical solution of the governing stability equations in the next section.

IV. RESULTS FROM NUMERICAL SOLUTION

A. Numerical method

We first briefly outline the numerical technique used to solve the governing equations and boundary conditions described in Sec. II C. There are two fourth-order ordinary differential equations (ODE) governing $\tilde{v}_z$ (for the liquid) and $\tilde{u}_z$ (for the solid). We first recast the fourth-order ODEs as a set of four first-order ODEs, and use a fourth-order Runge-Kutta integrator with adaptive step size control to numerically integrate the set of first-order ODEs [17]. To carry this out in the solid layer, we must specify "initial conditions" for the function $\tilde{u}_z$ and its first three derivatives at a given value of the independent variable z. For the solid layer at $z=(1+H)$, we have the zero displacement conditions: $\tilde{u}_z=0$ and $\tilde{u}_x=\mathrm{i}/kd_z\tilde{u}_z=0$. We use two different (linearly independent) sets of higher derivatives $d_z^2\tilde{u}_z=(1,0)$ and $d_z^3\tilde{u}_z=(0,1)$ at $z=(1+H)$ and numerically integrate the differential equation (21) up to $z=1$. This yields two linearly independent solu-

tions to the displacement field consistent with the two zero displacement conditions at $z=(1+H)$ in the solid layer. Corresponding to these two linearly independent solutions, we evaluate the velocity field of the fluid $\tilde{v}_z$ and its higher derivatives from the interfacial conditions at $z=1$ [Eqs. (25)–(28)]. Using these two sets of values for $\tilde{v}_z$ and its derivatives, we integrate the differential equation (17) in the fluid from $z=1$ to $z=0$. The velocity field in the fluid is obtained as a linear combination of these two solutions. At $z=0$, the fluid velocity field must satisfy the free-surface conditions (23) and (24). This is written in a matrix form, and the determinant of this matrix is set to zero to obtain the characteristic equation. This is solved numerically using a Newton-Raphson iteration procedure to obtain the eigenvalue c, for specified values of Γ, Re, k, β, H, Σ, and η_r. We use the low-k asymptotic results as a starting guess for the numerical procedure, and continue the low-k results numerically to finite values of k. The results from the numerical method were first validated by comparing it with the predictions of the asymptotic analysis, and excellent agreement was found.

B. Results

There are several objectives behind our numerical solution of the governing stability equations for the coupled fluid-solid problem. First, it is of interest to enquire if the predicted stabilization using long-wave analysis continues to perturbations with finite wavelengths. Second, stabilization of the free-surface instability is achieved when Γ is increased beyond a critical value. If Γ is further increased, there is possibility of the interface between the liquid and the deformable solid to become unstable. The instability of the liquid-solid interface was first analyzed, to the best of our knowledge, by Kumaran *et al.* [10] for plane Couette flow past a deformable solid, and they showed that the interface becomes unstable at finite wavelengths when Γ increases beyond a particular value. Consequently, will there be a sufficient "window" in the parameter Γ (equivalently, the shear modulus G for fixed values of other parameters) where the free-surface instability is stabilized, but the liquid-solid interface instability is not excited? We address these issues using the numerical solution. For ease of reference, we refer to the free-surface (liquid-gas) interfacial mode as "mode 1" and the liquid-solid interfacial mode as "mode 2" in the following discussion. To obtain the numerical results for mode 1, we use the low-k asymptotic results from the preceding section as a starting guess, and use the numerical procedure outlined above to continue the low-k results to finite values of k. For mode 2 instability, which happens at finite k, we use a Re=0 analysis (similar to [10], where analytical solution is possible for arbitrary k), to identify the presence of the unstable liquid-solid interfacial mode. The Re=0 results are then numerically continued to the desired finite Re.

Figure 4 shows the variation of the imaginary part of the wave speed c_i as a function of the wave number k for different values of Γ for $\beta=\pi/4$ and Re=1. When $\Gamma=0$ (rigid inclined plane), c_i is positive (mode 1 unstable) from $k \ll 1$ to $k \sim 0.4$, and for larger values of k the system is stable. As Γ is increased to 0.5 and 2, the instability is suppressed by the solid layer at all wave numbers. Here, we have set the nondimensional surface tension $\Sigma=0$, since even the flow down a rigid inclined plane is stable for $k>0.4$. (The only role of nonzero surface tension Σ is to stabilize short wavelength perturbations, if they are unstable.) However, as Γ is further increased to 5.5 (see Fig. 5), we find that perturbations with $k \sim 1$ are destabilized by the deformability of the solid layer. Thus, it is seen that when Γ is not too high, the free-surface

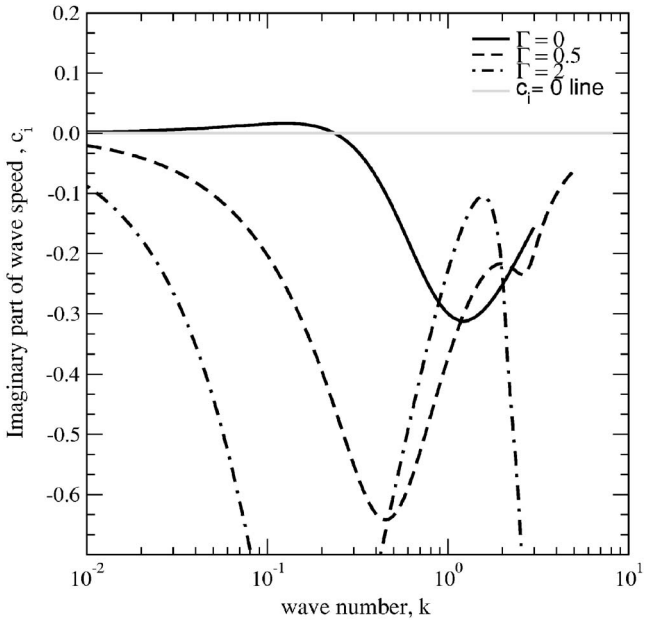

FIG. 4. Stabilization of mode 1 by the deformable solid layer: c_i vs k for $\beta=\pi/4$, Re=1, $H=0.5$, $\eta_r=0$, $\Sigma=0$, and different values of Γ.

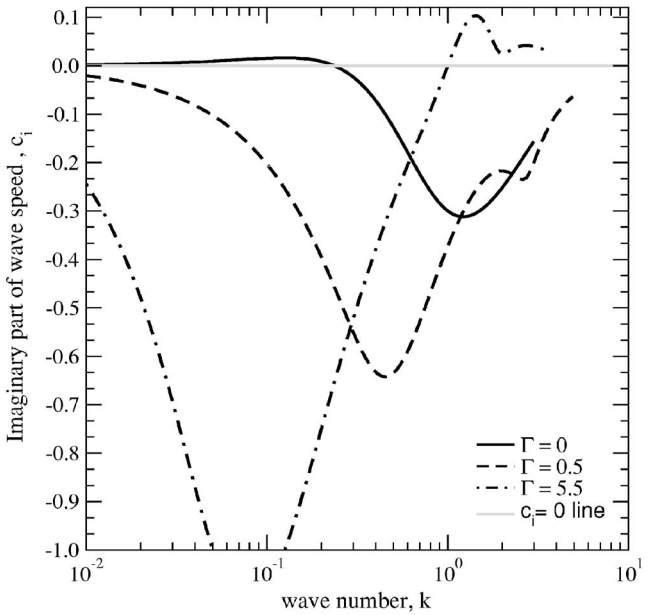

FIG. 5. Destabilization of finite-k waves of mode 1 by the solid layer at higher values of Γ: c_i vs k for $\beta=\pi/4$, Re=1, $H=0.5$, $\eta_r=0$, $\Sigma=0$.

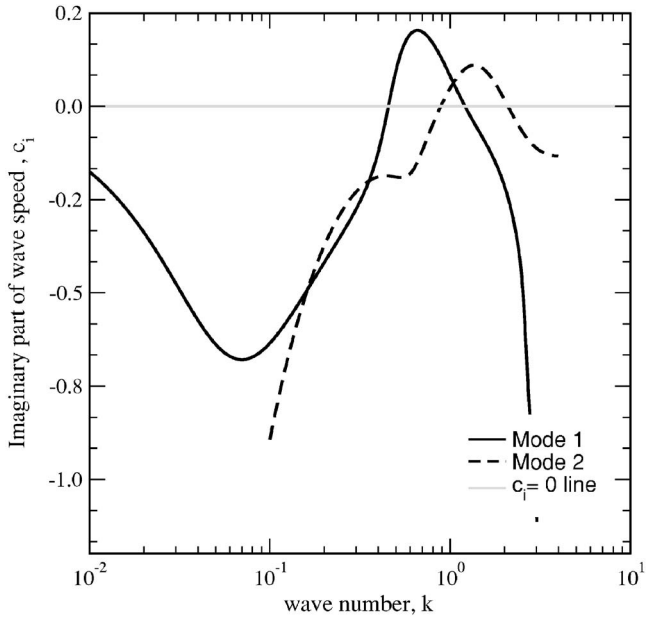

FIG. 6. Destabilization of finite-k waves of both modes 1 and 2 by the solid layer: c_i vs k for $\beta=\pi/4$, Re=1, $\Gamma=1$, $H=2$, $\eta_r=0$, $\Sigma=0$.

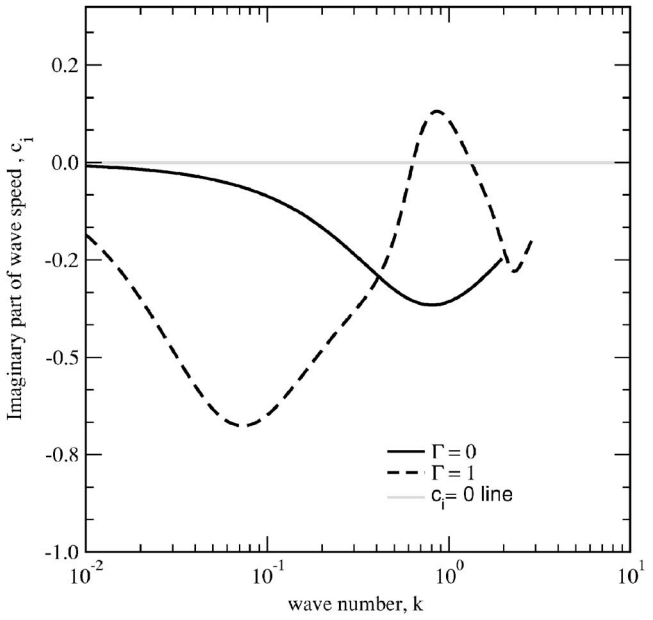

FIG. 7. Destabilization of mode 1 at finite k by the solid layer when it is stable in a rigid channel: c_i vs k for $\beta=\pi/4$, Re=0.1, $H=2$, $\eta_r=0$, $\Sigma=0$.

(mode 1) instability is completely suppressed at all wave numbers, but at higher values of Γ, mode 1 is destabilized at finite k, while perturbations with such wavelengths are stable in a rigid inclined plane. For the value of H chosen in these two figures, we did not observe any mode 2 instability.

As H is increased from 0.5 to 2 in Fig. 6, we observe that there are two different unstable modes at finite k, where both modes 1 and 2 become unstable at this value of $\Gamma=1$. However, when Γ is decreased, both these finite-k unstable modes become stable. In Fig. 7, we consider Re=0.1 and $\beta=\pi/4$, and in this configuration, there is no mode 1 instability in flow down a rigid inclined plane (as Re=0.1 is not large enough). We examine the effect of solid-layer deformability on this configuration in Fig. 7, and this shows that as Γ is increased, while waves with low k still remain stable, waves with finite k do become unstable. This shows that as Γ is increased further, there is always a deformability-induced free-surface instability at *finite* wavelengths. Our discussion thus shows that as Γ is increased from 0 there is a stabilization of mode 1 by the deformable solid layer at all wavelengths, when Γ increases beyond a critical value as given by the long-wave asymptotic analysis [Eq. (66)]. When Γ is further increased, much higher than the critical value for stabilization of mode 1, in general, this has a *destabilizing* effect on finite-k waves of both modes 1 and 2.

The above results pertain to Re$\leqslant 1$. When Re is increased to 10 (Fig. 8), it is seen that regardless of the value of Γ, there is always a finite-k mode 1 instability induced by the deformable solid layer. Thus, at higher Re, the deformable solid layer has a stabilizing effect only on perturbations with low k, and it has a destabilizing effect on finite-k perturbations. The results presented thus far are for the growth rate (proportional to c_i) vs wave number for a fixed value of Γ. It is useful to present the stability results in terms of a "neutral stability diagram" in the Γ-k plane where stable and unstable regions are demarcated. This will aid in selection of nondimensional parameters where the solid layer has completely suppressed the mode 1 instability at all wavelengths; such estimates can then be used in experimental studies to verify the present theoretical predictions.

Figure 9 presents the neutral stability diagram for Re=1, $\beta=\pi/4$, and $H=0.5$. Recall that $\Gamma=0$ is the limit of a rigid solid layer, and in that limit, the free-surface is unstable for

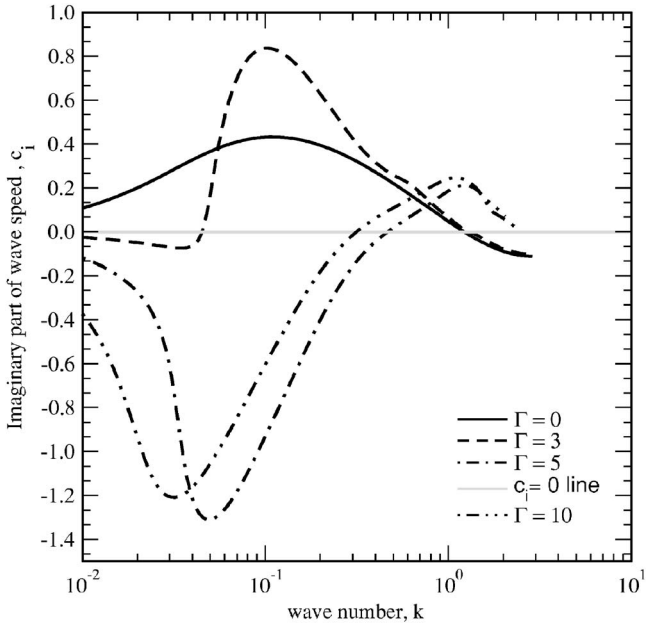

FIG. 8. Effect of solid layer deformability on mode 1 at Re =10: Illustration of finite-k instability at all values of Γ for $\beta=\pi/4$, $H=0.5$, $\eta_r=0$, and $\Sigma=0$. Stabilization of waves at all k is not possible for any value of Γ.

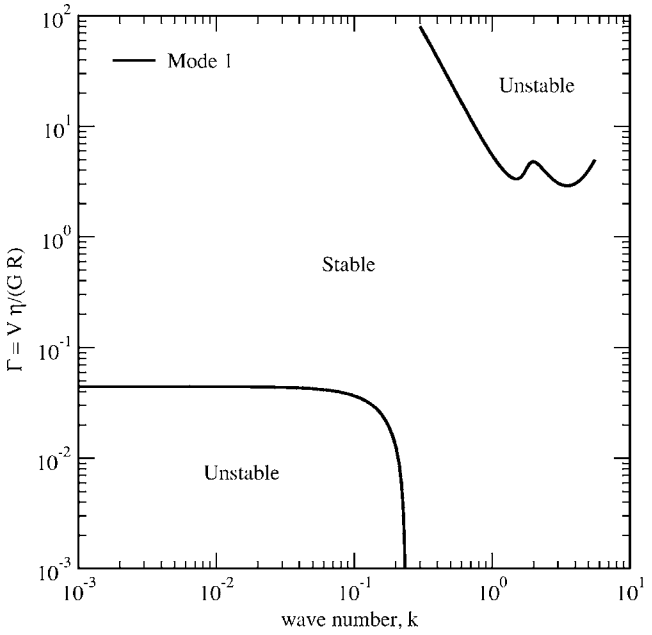

FIG. 9. Neutral stability curve for mode 1 instability in the Γ-k plane: $\beta=\pi/4$, Re=1, $H=0.5$, $\eta_r=0$, and $\Sigma=0$. Mode 2 instability is absent for this configuration.

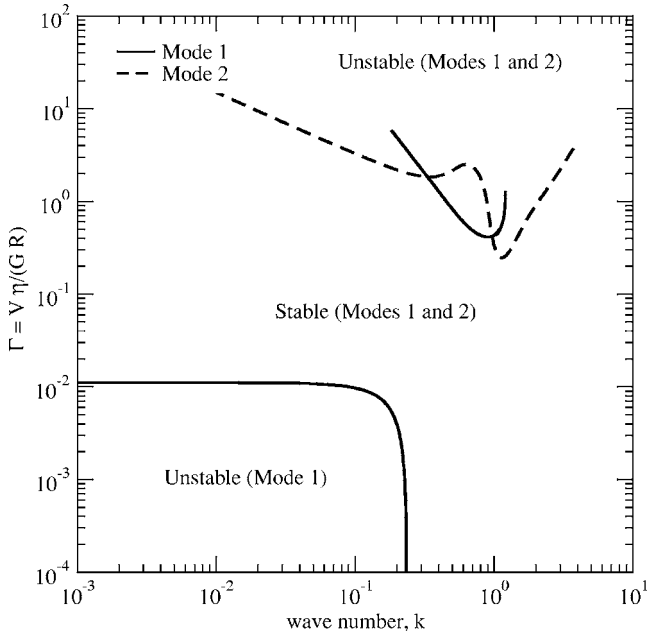

FIG. 10. Neutral stability curves for modes 1 and 2 in the Γ-k plane: $\beta=\pi/4$, Re=1, $H=2$, $\eta_r=0$, and $\Sigma=0$. At finite k, and at sufficiently higher values of Γ, the fluid-solid interfacial mode also becomes unstable, apart from the destabilization of the free-surface mode at finite k by the deformable solid layer.

$k \leqslant 0.4$ (also see the c_i vs k curve in Fig. 4). As Γ is increased beyond the lower neutral curve, there is a transition from unstable to stable perturbations of mode 1. There is a large region in Γ (for fixed values of other parameters, this translates into a large region in the shear modulus of the solid layer) where mode 1 is stabilized by the solid-layer deformability. As Γ is increased further, there is another neutral curve at finite k where there is a transition from stable to unstable perturbations. Our analysis did not show any mode 2 instability for the chosen value of $H=0.5$. As H is increased to 2 (Fig. 10), it is seen that there is a lower neutral curve for mode 1 which indicates that mode 1 is stabilized as Γ is increased beyond it, and there are two neutral curves at higher values of Γ and at finite k. These two neutral curves correspond to the destabilization of both mode 1 and mode 2 due to an increase in Γ at finite k.

The low-k asymptotic analysis indicated that the solid-fluid viscosity ratio η_r is subdominant in that limit, and hence does not affect the stabilization at low k. In Fig. 11, we examine the effect of increase in η_r on the neutral stability diagram presented in Fig. 9. This shows that an increase in η_r has virtually no effect on the lower neutral curve, but has a stabilizing effect on the upper neutral curve. Thus, nonzero η_r further increases the gap between the two neutral curves, and hence increases the region where mode 1 is completely suppressed. While the results presented above are for $\beta=\pi/4$, Fig. 12 illustrates that a similar suppression is expected even for $\beta=\pi/6$. Here, mode 1 instability is suppressed as Γ is increased beyond the lower neutral curve, and mode 2 instability is excited when Γ is increased beyond the upper neutral curve.

In Fig. 13, we present the neutral stability curves for $\beta=\pi/2$ (vertical-wall configuration). Let us first focus on the results for the case of surface tension $\Sigma=0$. For this case, we find that there are two different neutral curves for modes 1 and 2 at lower values of k, but as k approaches 1, both these neutral curves merge with one another. The region where both modes 1 and 2 are stable is confined only up to $k=1$, after which there is an instability of either mode 1 or mode 2.

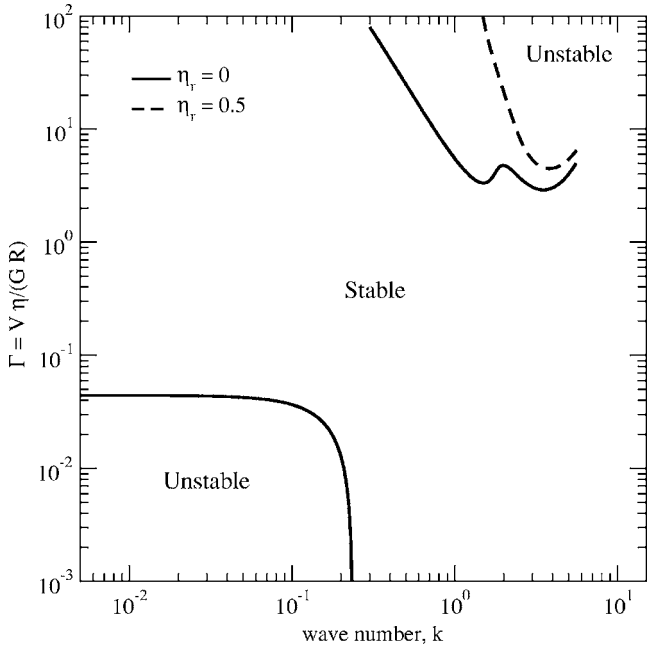

FIG. 11. Effect of the solid-layer viscosity η_r on the neutral stability curves in the Γ-k plane: $\beta=\pi/4$, Re=1, $H=0.5$, and $\Sigma=0$. While η_r has negligible effect on the lower neutral curve, it has a stabilizing effect on the upper neutral curve at finite k.

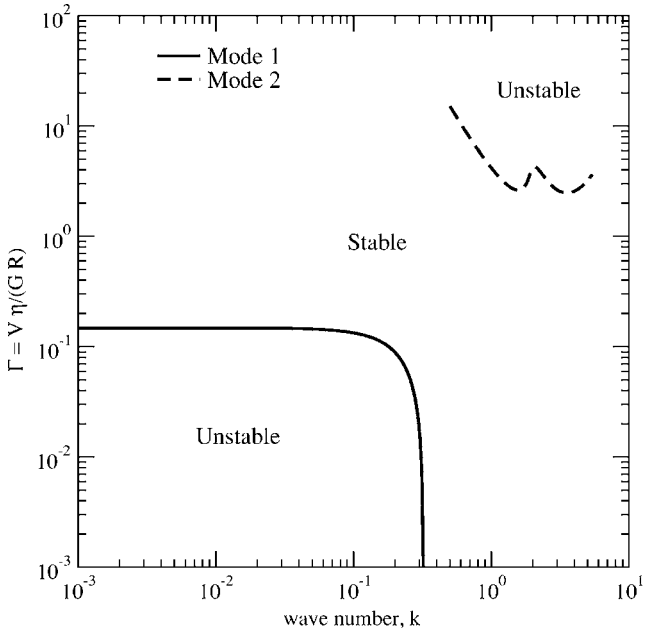

FIG. 12. Neutral stability curve illustrating the suppression of mode 1 instability for $\beta=\pi/6$, Re=2, $H=0.5$, $\eta_r=0$, and $\Sigma=0$. This figure illustrates the stabilizing effect of the solid layer on mode 1 and the destabilization at finite-k of mode 2 at higher values of Γ.

However, upon increasing the liquid-gas surface tension Σ to 0.1, we find that the neutral curves for modes 1 and 2 are separated, and in this case there is a range of values (about two orders of magnitude) of Γ where both the modes are stable for all values of k. Our numerical results, therefore, show that it is possible to choose the shear modulus of the solid layer so that the nondimensional parameter Γ is in the stable range for perturbations with all wavelengths.

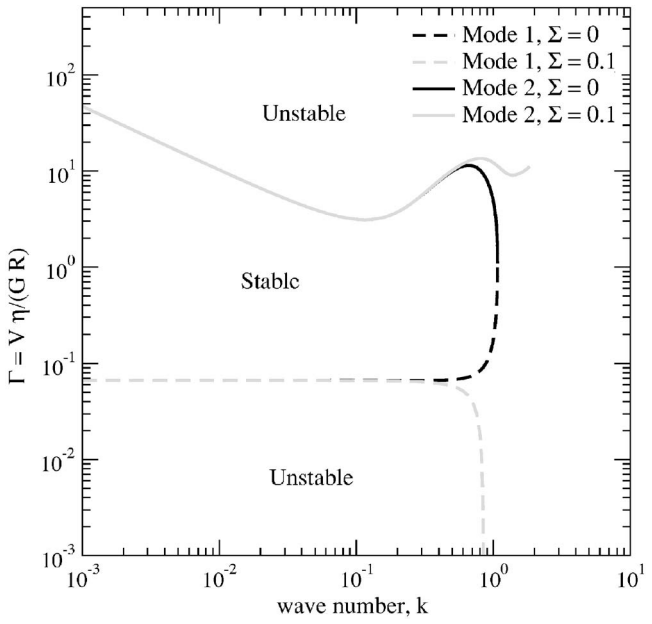

FIG. 13. Effect of liquid-gas surface tension Σ on the neutral curves for $\beta=\pi/2$, Re=0.1, $H=0.2$, $\eta_r=0$. This figure illustrates the "merging" of the two modes for $k\sim 1$ in the absence of surface tension, and the 'splitting' of the two modes with surface tension.

It is appropriate here to remark on the validity of the use of a simple linear viscoelastic model for the deformable solid layer in the present study. The nondimensional base-state strain in the solid layer is proportional to Γ, and strictly speaking, the use of the linear solid model is valid only when $\Gamma \ll 1$. The earlier study of Gkanis and Kumar [16] which used the neo-Hookean model for the solid for the stability of plane Couette flow past a deformable wall has shown, however, that in practice the predictions of the linear solid model remains accurate for $\Gamma \sim 1$, when $H \geqslant 2$ for the interfacial mode (mode 2) between the fluid and the solid layer. Our results for the stabilization of the free-surface mode (mode 1) shows that $\Gamma \sim 10^{-3}-10^{-2}$ for achieving this effect. Therefore, the present predictions for the stabilization of mode 1 are expected to be accurate despite the use of a linear solid model, since the Γ required to realize these effects is very small compared to unity. However, the use of a more complex constitutive relation for the solid layer will have some quantitative effect on mode 2 neutral curves, and the linear model is expected to be accurate for only $H \geqslant 2$. It must be mentioned that in applications where one might use a soft solid layer to stabilize the free-surface instability, it might be advantageous to use solid layers with smaller thickness with $H \leqslant 1$. In such cases of small solid layer thickness, the predictions of the linear solid model for mode 2 must become less accurate, and it may be desirable to use a nonlinear solid model, similar to Gkanis and Kumar [16].

V. SUMMARY AND CONCLUSIONS

The effect of the solid layer deformability on the free-surface instability in liquid film flow down an inclined plane lined with a soft solid layer was analyzed first using a long-wave asymptotic analysis, and then using a numerical solution of the governing stability equations. In the absence of the soft solid layer, the liquid film flow undergoes a long-wave instability due to fluid inertia. The present asymptotic results show that the effect of the solid layer appears at the same order $[O(k)]$ as the destabilizing effect of fluid inertia, but the deformability of the solid layer always has a stabilizing effect on the free-surface instability in the long-wave limit. Physically, at leading order in the asymptotic analysis, the normal and tangential fluid velocity fields satisfy the no-slip condition (as in a rigid inclined plane), and so the leading-order wave speed $c^{(0)}$ remains the same as in a rigid inclined plane. However, the leading-order fluid velocity field exerts a tangential stress on the solid layer, causing a deformation in the solid. This leading-order deformation in the solid layer affects the first correction to the fluid velocity field, thereby qualitatively altering the nature of the free-surface instability. For a fixed value of Re and the inclination angle β, the free-surface instability is stabilized when $\Gamma = V_a\eta/(GR)$ increases beyond a critical value. The long-wave asymptotic results are further extended to finite wavelengths using a numerical solution of the stability equations. In general, this shows that the suppression of the free-surface instability continues to finite wavelengths. However, an increase in Γ substantially away from the value required for

stabilization of the free-surface instability results in destabilization of either the liquid-solid interfacial mode or the free-surface interfacial mode at *finite wavelengths*. Representative numerical results presented for a variety of parameter regimes indicate, nevertheless, that there exists a wide range of values of Γ (typically two orders of magnitude) where both the interfacial modes are stabilized at all wave numbers. Furthermore, the suppression of instability for all wavelengths is found to be valid only for $\mathrm{Re} \sim O(1)$; when the Reynolds number is increased to 10 (for $\beta = \pi/4$), it was found that there was always a finite-wavelength instability induced by the deformable solid layer.

There are several implications from the present study for future experimental investigations. First, as discussed in Sec. III B, the predicted stabilization can be realized in experiments involving the flow of viscous liquids (viscosity $\sim 1 - 10$ Pa s) past a soft elastomeric solid layer (shear modulus $\sim 10^4$ Pa). Secondly, by decreasing the angle of inclination β, it is possible to verify the destabilizing effect of solid-layer deformability on the free-surface instability at finite wavelengths, when there is no long-wave instability in liquid flow down a rigid inclined plane. Thirdly, while the present study was restricted to the realm of linear stability, the nonlinear dynamics of liquid flow past an inclined plane lined with a soft solid layer could also potentially be qualitatively different from that of a rigid inclined plane. For example, it might be expected that the nonlinear evolution of the finite-wavelength instability due to the deformability of the solid layer could be very different from that of the long-wave instability of liquid flow down a rigid inclined plate. This is an issue that is worth studying in future experimental and theoretical investigations. In conclusion, the present study predicts a discernible consequence of the elastohydrodynamic coupling between the liquid flow and the deformation in the soft solid on the free-surface instability of falling liquid films which can be readily tested by experiments.

[1] H. -C. Chang and E. A. Demekhin, *Complex Wave Dynamics on Thin Films* (Elsevier, Amsterdam, 2002).
[2] T. B. Benjamin, J. Fluid Mech. **2**, 554 (1957).
[3] C. -S. Yih, Phys. Fluids **6**, 321 (1963).
[4] J. B. Grotberg and O. E. Jensen, Annu. Rev. Fluid Mech. **36**, 121 (2004).
[5] E. S. G. Shaqfeh, R. G. Larson, and G. H. Fredrickson, J. Non-Newtonian Fluid Mech. **21**, 87 (1989).
[6] H. -H. Wei, Phys. Fluids **17**, 012103 (2005).
[7] H. -H. Wei, Phys. Rev. E **71**, 066306 (2005).
[8] S. P. Lin, J. N. Chen, and D. R. Woods, Phys. Fluids **8**, 3247 (1996).
[9] W. Y. Jiang and S. P. Lin, Phys. Fluids **17**, 054105 (2005).
[10] V. Kumaran, G. H. Fredrickson, and P. Pincus, J. Phys. II **4**, 893 (1994).
[11] V. Kumaran and R. Muralikrishnan, Phys. Rev. Lett. **84**, 3310 (2000).
[12] V. Shankar and L. Kumar, Phys. Fluids **16**, 4426 (2004).
[13] L. Landau and E. Lifshitz, *Theory of Elasticity* (Pergamon, New York, 1989).
[14] V. Shankar and V. Kumaran, J. Fluid Mech. **408**, 291 (2000).
[15] V. Shankar and V. Kumaran, Phys. Fluids **14**, 2324 (2002).
[16] V. Gkanis and S. Kumar, Phys. Fluids **15**, 2864 (2003).
[17] P. Drazin and W. Reid, *Hydrodynamic Stability* (Cambridge University Press, Cambridge, 1981).